# Free-Energy Profile for CO Binding to Separated Chains of Human and *Trematomus newnesi* Hemoglobin: Insights from Molecular Dynamics Simulations and Perturbed Matrix Method

**Antonello Merlino,*[,†,‡] Alessandro Vergara,[†,‡] Filomena Sica,[†,‡] Massimiliano Aschi,[§] Andrea Amadei,[∥] Alfredo Di Nola,[⊥] and Lelio Mazzarella[†,‡]**

*Dipartimento di Chimica, University of Naples "Federico II", Complesso Universitario Monte S. Angelo, Via Cinthia, I-80126 Naples, Italy, Istituto di Biostrutture e Bioimmagini, CNR, Via Mezzocannone 16, I-80134 Naples, Italy, Dipartimento di Chimica, Ingegneria Chimica e Materiali, University of L'Aquila, Via Vetoio, I-67010, L'Aquila, Italy, Dipartimento di Scienze e Tecnologie Chimiche, University of Rome "Tor Vergata", Via della Ricerca scientifica 1, I-00133 Roma, Italy, and Dipartimento di Chimica, University of Rome "La Sapienza", P.le Aldo Moro 5, I-00185 Roma, Italy*

*Received: September 3, 2009; Revised Manuscript Received: March 5, 2010*

The free-energy profile and the classical kinetics of the heme carbomonoxide binding−unbinding reaction have been derived by means of a theoretical method for the separated chains of human (HbA) and *Trematomus newnesi* major component (HbTn) hemoglobin. The results reveal that the α- and β-chains of HbA have similar values of kinetic constants for the dissociation of the Fe−CO state, in agreement with experimental data. Comparisons of the present findings with the data obtained for the α- and β-chains of HbTn and with theoretical and experimental results previously collected on myoglobin provide a detailed picture of this important biochemical reaction in globins. The sequence and structural differences among the globins are not reflected in meaningful variations in the rate of CO dissociation. These data support the conclusion that the differences observed for the reaction with CO of globins, if any, involve the rate of ligand migration to the solvent, rather than the Fe−CO complex formation/rupture. Furthermore, our results agree with the recent discovery that globin family proteins exhibit common dynamics, thus confirming the observation that the dynamic properties of proteins are strongly related to their overall architecture.

## Introduction

The heme group, a planar organic molecule with a central iron atom, plays a central role as an active center in biomolecules performing functions that range from oxygen storage to redox reactions and catalysis. The binding and release of a small ligand with the iron of a heme buried within a compact protein is one of the simplest and most fundamental chemical reactions taking place in living organisms. The globin family is an important model system for these reactions. Hemoglobins (Hbs) are the most prominent members of the globin family. These molecules are widely distributed in all living organisms including animals, plants, bacteria, and yeasts. Hbs are tetrameric molecules composed by the assembly of two identical α−β heterodimers, in which each subunit carries a heme group to which oxygen, carbon monoxide, and other ligands bind reversibly. Hb is traditionally thought to assume two different tetrameric conformations, T or tense, characterized by a low affinity for the ligand and typical of the unliganded form, and R or relaxed, with high affinity and typical of the ligated form,[1] but recent crystallographic analyses have clearly shown that a wider variety of structural states are accessible to Hb.[2−5]

When the α- and β-chains of human Hb (HbA) are isolated, their structural properties are similar and resemble those of natural HbA.[6,7] However, some features are different: the ligand affinity is greatly increased, and subtle modifications in heme pockets are observed.[6] Although distinctions between the α- and β-chains are subtle, they are discernible by a variety of techniques: the two subunits show differences in exchangeable hydrogens, in the visible adsorption spectrum and in the CD spectrum.[8−10] Furthermore, individual α- and β-chains are more unstable than tetrameric HbA, and the α-globin is more unstable than β-globin.[9,11] The β-chains can form dimers and tetramers that are more stable than the monomeric form, whereas the α-chain is preferentially monomeric, although it can form unstable dimers.[9,11]

Many experimental studies have been performed to determine affinity and kinetic constants of the ligand binding reaction for the separated chains of HbA and for each chain within the tetramer, and a variety of results have been reported.[12−16] In this respect, interesting results have been obtained using CO as a probe.

First, studies suggested that CO migration into and out of the HbA subunits was different.[1] However, more recently it has been shown that there is a great similarity in the behavior of the α- and β-chains.[12,15] Indeed, Gibson and co-workers,[17] Hernan and Sligar,[18] and Unzai et al.[19] demonstrated that the α- and β-HbA chains have similar affinities for CO (differences in free energy is less than 2 kJ/mol) and are similar to those of intact hemoglobin. The α- and β-subunits in both R and T states show roughly equal CO association rate constants and only slightly different dissociation rate constants.[19] In particular, in the R-state the association rate constant is about 6 $\mu M^{-1}$ $s^{-1}$

* To whom correspondence should be addressed. Fax: +39081 674090. Tel.: +39081 674276. E-mail: antonello.merlino@unina.it.
† University of Naples "Federico II".
‡ Istituto di Biostrutture e Bioimmagini.
§ University of L'Aquila.
∥ University of Rome "Tor Vergata".
⊥ University of Rome "La Sapienza".

10.1021/jp908525s 
Published on Web 04/30/2010

for the α-chain and β-chain, whereas in the T-state it is 0.16 $\mu M^{-1}$ $s^{-1}$ for the α-chain and 0.07 $\mu M^{-1}$ $s^{-1}$ for the β-chain. The $k_{off}$ is in the range 0.005−0.012 $s^{-1}$ for the α-chain and 0.007−0.011 $s^{-1}$ for the β-chain.

Recently, theoretical methods have been successfully used to study the members of the globin family,[20−23] and the influence of the molecular structure on the energetics of the quintet and singlet states of the heme has been reported.[21] The Perturbed Matrix Method (PMM)[20] combined with extended molecular dynamics sampling has been used to characterize the kinetics of heme CO binding/unbinding in myoglobin.[24]

Here, we report a study of the CO binding/unbinding to the separated chains of HbA and of the major Hb isolated from the Antarctic fish *Trematomus newnesi* (HbTn chains). The comparison between HbA and HbTn chains is interesting, as it has been proved that these Hbs exhibit different structural and biophysical properties[25−27] in their carbomonoxy state. In particular, recent studies have revealed that the two proteins have large differences in their auto-oxidation pathway starting from the CO form:[28,29] HbTn oxidation leads to the formation of species such as bishistidyl adducts and pentacoordinated states, whereas HbA essentially oxidizes to aquo-met forms. Notably, the oxidation leads to the formation of the bishistidine only in the β-subunit of HbTn.

The results of this study have been compared with available experimental data and with previous results collected on myoglobin.

## Methods

**System and Definitions.** HbA is a globular protein with a molecular mass of 64.5 kDa containing two α and two β globin chains, each one associated with a heme prosthetic group. The two chains are very similar in overall conformation but differ substantially in amino acid sequence.[30] The α chain has 141 residues and the β chain 146 residues. The number of residue differences is 47. The structure of both the α- and β-chain closely resembles that of myoglobin.[30,31] It consists of eight tightly packed helices. The six major and the two short α-helices that make up the structure of each chain (globin fold) are labeled A through H, according to the traditional naming scheme. The helices form an approximately cylindrical bundle, with the heme and its central iron atom bound in a hydrophobic pocket between helices E and F. The main difference between the α- and β-chain is the lack of helix D, replaced by a loop in the α-chain.

HbTn structure is similar to that of HbA. The α-chain has 142 residues and the β-chain 146 residues. The main differences between the HbA and HbTn structure are located at the CDα region, where the fish Hb has an insertion of a proline in position 47 and at the N-terminal Ser that is acetylated in HbTn.

**MD Simulations.** All the computer simulations reported in this study were performed using GROMACS 3.2 package[32] and the GROMOS96 force field. The α- and the β-chain models for HbA and HbTn have been taken from the X-ray structures of the CO-bound forms of the two proteins solved at 1.25[33] and 2.20 Å[34] resolution, respectively. The starting models were immersed in a box containing about 7500 simple-point-charge[35] water molecules. The ionization state was set to mimic a neutral pH environment. The overall charge of the systems was neutralized by adding the appropriate number of ions more than 7 Å away from the protein surface. In the first step of the equilibration process, the solvent was relaxed by energy minimization followed by a 20 ps MD at 300 K. The overall system was then minimized without restraints, before the productive run, and 23−25 ns for each system have been collected. We used the last 20 ns of the trajectories for the analyses. All bond lengths were constrained by LINCS;[36] Newton's equations of motion were integrated with a time step of 2 fs, and atomic coordinates were saved for analyses every 0.5 ps. A dielectric constant of 1 was used. The Part Mesh Ewald method (PME)[37] was used for the treatment of electrostatic interactions for atoms at a distance greater than 9 Å. All systems were simulated in the NVT ensemble at 300 K using periodic boundary conditions in the three coordinate directions and constraining the molecule in the center of the simulation box. The temperature was kept constant using the Berendsen thermostat with a coupling constant $\tau_p = 1$ fs.[38] The parameters describing the His-Heme-CO force field used in the simulation are those previously reported.[24]

To determine the equilibrated portion of the trajectories, essential degrees of freedom for the two chains of HbA and HbTn were extracted from the two trajectories according to the essential dynamics method,[39−43] and the overlap of the essential spaces of each ensemble was evaluated by using the rmsip, as previously suggested.[40−44] The convergence in the essential space (first 10 eigenvectors) was checked by using the root-mean-square inner product (rmsip) between two halves of the equilibrated trajectory.[40−44]

In particular, the rmsip is defined as

$$\sqrt{\frac{1}{10}\sum_{i=1}^{10}\sum_{j=1}^{10}(v_i^a v_j^b)^2}$$

where $v_i^a$ and $v_j^b$ are the $i$th and $j$th eigenvectors from the first and second half of the equilibrated trajectory, respectively. Only $C^\alpha$ atoms were included in the definition of the covariance matrices for the enzyme.

**Perturbed Matrix Method and Kinetic Modeling.** The computational details of PMM and kinetic modeling have been fully described by Amadei et al.[24] In the present paper, only some relevant aspects will be recalled. PMM is a perturbative approach whose basic approximation is the possibility to define a subportion of the simulated system to be explicitly treated at the electronic level, hereafter termed as quantum center (QC), with the rest of the system—typically the rest of the protein and the solvent—acting as a classical perturbation.

Briefly, the perturbed QC Hamiltonian matrix $\tilde{H}$ on the Born−Oppenheimer (BO) surface is defined as

$$\tilde{H} \cong \tilde{H}^0 + q_T \mathcal{V}\tilde{I} + \tilde{Z}_1 + \Delta V\tilde{I} \quad (1)$$

where $\tilde{H}^\circ$ is the unperturbed QC Hamiltonian matrix constructed in the present study via configuration interaction calculations with single and double excitations (CISD), including the ground state plus nine excited states; $q_T$ is the QC total charge; $\mathcal{V}$ is the perturbation electric potential exerted by the environment on the quantum center; $\tilde{Z}$ is the perturbation matrix provided by the inner products between the unperturbed transition dipoles and the perturbing electric field; and $\Delta V$ approximates the perturbation due to all the terms from the quadrupoles on as a simple short-range potential. It is worth noting that, at each MD frame, the electric potential and field exerted by the environment can be calculated and the perturbed Hamiltonian matrix diagonalized. Hence, a trajectory of the perturbed eigenvalues and eigenvectors is obtained. Such a calculation, if carried out along predefined reaction coordinates, provides the free energy change ($\Delta A$)

$$\Delta A \cong -kT \ln\langle e^{-\beta\Delta(\varepsilon' + q_T \mathcal{V})}\rangle^0_{\eta_a} \quad (2)$$

In the previous equations, $\Delta(\varepsilon' + q_T \mathcal{V})$ provides the energy change, for each MD frame, due to the transition along the reaction coordinates, and $\eta_a$ is the position of the reaction coordinates used to obtain the statistical ensemble, i.e., used in the MD simulation. Moreover, the subscript $\eta_a$ and the zero superscript of the averaging operator mean that the average is taken in the statistical ensemble where the reaction coordinates are constrained at $\eta_a$. The perturbing electric field, used to construct the perturbed Hamiltonian matrix utilized in PMM, was obtained at each MD configuration by the atomic charges within the simulation box (excluding QC charges).

We utilized the same reaction center (the quantum center, Figure 1) of the previous article,[24] defined by the isolated His-Heme−CO complex. The calculations have been done using Gaussian98[45] and GamessUS packages.[46] The computational level, the force field, and the specific parametrization for the internal degrees of freedom of heme used in this paper have been tested in many other works[20,24] and references therein. The reaction coordinate, i.e., the iron−carbon distance, was used to define a six-point grid starting from the unperturbed potential energy minimum (located at 1.8 Å on the singlet surface) up to 3.8 Å. The same approach was adopted for the three magnetic states, i.e., singlet, quintet, and triplet.

Such a scan was carried out using Density Functional Theory adopting the B3LYP functional[47] in conjunction with the following basis set: Hay and Wadt Effective Core Potential (ECP)[48] for iron and double-ζ basis set for core and valence electrons, respectively; 6-311++G(d,p) basis set for the atoms directly connected to iron and for CO; and finally, 6-31G for the remaining atoms. Using the obtained eigenvectors, we have performed configuration interaction calculations only to construct the PMM-Hamiltonian. For the application of PMM at each point, the first nine excitation energies and transition dipoles were obtained using configuration interaction calculations including single and double excitation (CISD) using as a reference the Slater determinant, the one obtained by B3LYP calculations. These quantum chemical calculations are free of any assumption.

**Analysis of the Trajectories.** To determine local deviations from the starting structure, the root-mean-square deviation (rmsd) of the individual $C^\alpha$ atoms was computed as follows

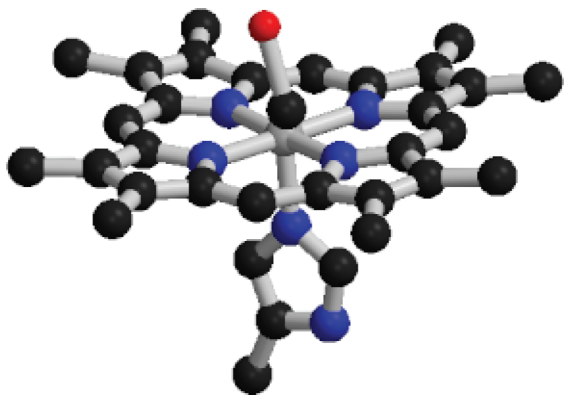

**Figure 1.** Schematic view of the quantum center used in our PMM calculation, defined by the heme−CO complex and including the proximal histidine side chain.

$$\text{rmsd: } \sqrt{\frac{1}{N}\sum_i^n (r_i - r_0)^2}$$

where $r_i$ represents the $C^\alpha$ position at time $i$ and $r_0$ the reference value.

The rmsd was also calculated using the recently derived reference set of fixed residues. In particular, residues 23−42, 57−63, 101−111, and 118−125 of the HbA α-chain and residues 51−57, 110−116, and 119−132 of the HbA β-chain have been compared to the same set of residues in the starting structure. A similar analysis has been performed on the α- and β-chains of HbTn.

Information on the mobility of each protein $C^\alpha$ atoms with respect to the average structure was derived by measuring the root-mean-square fluctuation (rmsf), as follows

$$\text{rmsf: } \sqrt{\frac{1}{N}\sum_i^n (r_i - \langle r\rangle)^2}$$

where $r_i$ represents the $C^\alpha$ position at time $i$ and $<r>$ the average value.

## Results

**Structural Stability.** Several time-dependent properties of the α- and β-chains of human and *Trematomus newnesi* major component hemoglobin were analyzed to ascertain the stability of the MD simulations. The root-mean-square deviation (rmsd) of the coordinates during the simulation versus the starting models as a function of time is reported in Figure 2. This plot shows that a plateau is reached after 3000 ps for the $C^\alpha$ atoms of each chain and that the simulated structures remain close to their starting models (rmsd < 2 Å). The time evolutions of the secondary structure elements, the total number of hydrogen bonds, and the radius of gyration (data not shown) indicate that the globins maintain the correct globular folding during the simulations.

To ensure that the structural and dynamic properties derived from the simulations are free from initial nonequilibrium effects, all the analyses were performed in the last 20 ns of the trajectory. In this region, the essential subspace converged as revealed by calculating the rmsip value (see Methods) between the two halves of the trajectory (rmsip values from 0.64 to 0.67), and the geometric parameters analyzed showed low standard deviations.

**Deviations and Fluctuations.** To characterize the differences between the simulated structure of α- and β-chains of HbTn and HbA and those of the starting models, we have computed the root-mean-square deviation (rmsd) between the average conformations obtained from the simulations and the structures of the α- and β-chains of HbA and HbTn within the tetramer. The overall structure of each chain closely matches that of the crystallographic structure (Figure 3). In HbA, the rmsd per residue shows that deviations from the starting models larger than 2.0 Å are located at the chain termini, between helices A and B, at the CE loop, at the end of helix E, and in the EF loop for the α-chain and between helices A and B, at the helix C, at the CD and EF loops, and at the C-terminal tail for the β-chain. In the Antarctic fish Hb, the highest deviations are located at the CE loop and at the termini for the α-chain, whereas they are more diffuse on the β-chain. In particular, the highest mobilities are observed at the CD, EF, and GH loops and at

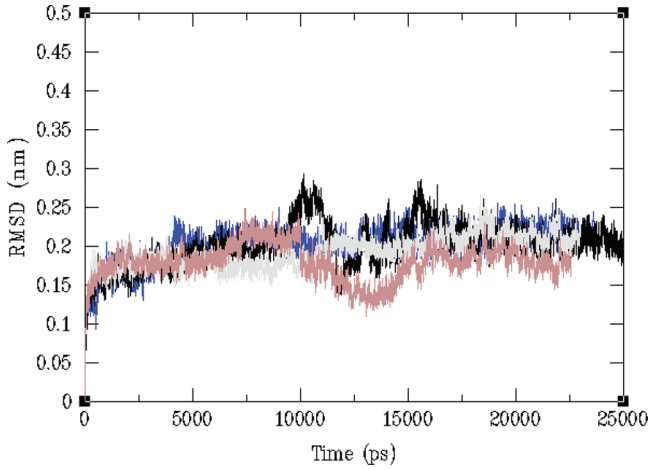


**Figure 2.** Time behavior of the root-mean-square positional deviations from the starting structures computed on $C^{\alpha}$ atoms for the α- and β-chain of HbA (black and gray lines) and HbTn (blue and light brown lines, respectively).

**Figure 3.** Ca atoms of the average structure derived from MD simulation of the β-chains of HbA (black line) superimposed to its starting model (gray line).

the residues 100−101 of helix G. These data are not surprising given that the most significant differences between the corresponding structures are located in flexible loops and/or in regions that in the X-ray structures are involved in the formation of intersubunit contacts.

The rmsd has also been used to ensure that the quantum center (QC) has a rather rigid structure. This finding ensures that at each point of the reaction coordinate we can evaluate the unperturbed basis set without spanning the internal fluctuations of QC. The QCs present low rmsd with a maximum value of 0.93 Å, after superimposition of all atoms.

The dynamics of the α- and β-chains of HbA and HbTn during the simulations have been also analyzed. The result indicates that the β-chains of HbTn and HbA share a similar flexibility that is generally greater than that of the α-chain, whereas the α-chain of HbTn is somewhat less flexible than that of HbA. For each structure, the root-mean-square fluctuation (rmsf) is larger in the loop regions and at the helix termini, whereas helical segments show a smaller mobility. Particularly, in the α-chain of HbA the most flexible regions are the N- and C-terminal residues, the EF loop, the region between helix A and B, and the beginning of helix C and of helix E (Figure 4A). In the β-chain of HbA, the most flexible regions are located at the chain termini, at the CD and EF loops, and at the helix C (Figure 4B).These data are in good agreement with the picture depicted by Ho and co-workers for the dynamics of the α- and β-chains of carbomonoxy tetrameric HbA.[49]

In the α-chain of HbTn, the most flexible regions are the loop residues 1−2, 49, and 143 (Figure 4C), whereas in the β-chain higher mobility is observed for the chain termini, at the CD and GH corners (Figure 4D).

**Free Energy Profile of CO−Heme Binding/Unbinding.** The free energy profile of the CO binding/unbinding to the α- and β-chains of HbA and HbTn as obtained by PMM and MD simulations is reported in Figure 5. As expected, the ligated singlet state is more stable than the quintet state, and the transition state of the reaction is determined by the crossing between the singlet and quintet surfaces. From the figure, it is evident that the free energy surfaces of the α- and β-chains of HbA and HbTn are strictly similar. The computations also indicate that the ligated α- and β-chains of the two hemoglobins have similar stabilities.

In Table 1, the free energy barriers obtained from the reaction free energy surface have been reported in comparison with the data obtained for myoglobin and with that obtained for the unperturbed QC reference state. The free energy barriers of the four Hb chains are almost identical. Furthermore, as observed for myoglobin,[24] each Hb chain has a catalytic effect, lowering the energy barrier with respect to the unperturbed state. The values obtained for the Hb chains are also similar to those previously reported for myoglobin. The energy difference ($\Delta E$ about 30 kJ/mol) between the electronic states when the iron is hexacoordinated (singlet) and when CO is dissociated (iron is pentacoordinated and in the quintet state) obtained using our approach is in reasonable agreement, within the noise, with the data obtained by other authors ($\Delta E = 9-19$ kcal/mol).[21]

**Rate Constants for CO Dissociation.** The calculated rate constant for CO dissociation ($k_{unb}$) of the four Hb chains is about 0.45 $s^{-1}$, corresponding to a half-life of a few seconds. This constant refers to the rupture of the Fe−CO covalent bond. Such results are comparable to those obtained for myoglobin at both 300[24] and 200 K (unpublished data). Assuming that the rupture of the Fe−CO bond is the rate-limiting step of the dissociation process, calculated $k_{unb}$ can be compared with the experimental rate for dissociation constants ($k_{off}$). Indeed, the $k_{unb}$ values calculated for α- and β-chains of human hemoglobin well agree with the dissociation constants $k_{off}$ available in the literature, obtained for the separated chains of HbA and for the chains within the tetramer (Table 2) (note that only a few tenths of kilojoules/mole variation in the unbinding barrier would account for about 40 times variation of $k_{off}$). No experimental data are available for the separated chains of HbTn.

## Discussion

The binding and release of small ligands in proteins is a crucial step in several important biochemical reactions. The binding of CO to the ferrous form of myoglobin and hemoglobins is perhaps among the most studied reactions taking place in living organisms. Besides the basic interest in the understanding of this molecular process, it should be recalled that CO is produced in vivo as a second messenger for regulating various physiological functions including blood pressure, platelet aggregation, and neurotransmission, and thus this reaction has an important physiological role.

The overall features of the CO binding to myoglobin, isolated heme group, and separated Hb chains possess striking similarities. Access to the heme pocket is governed by sequential barriers. Various theoretical models have been hypothesized to explain the existence of the barriers. The most commonly used

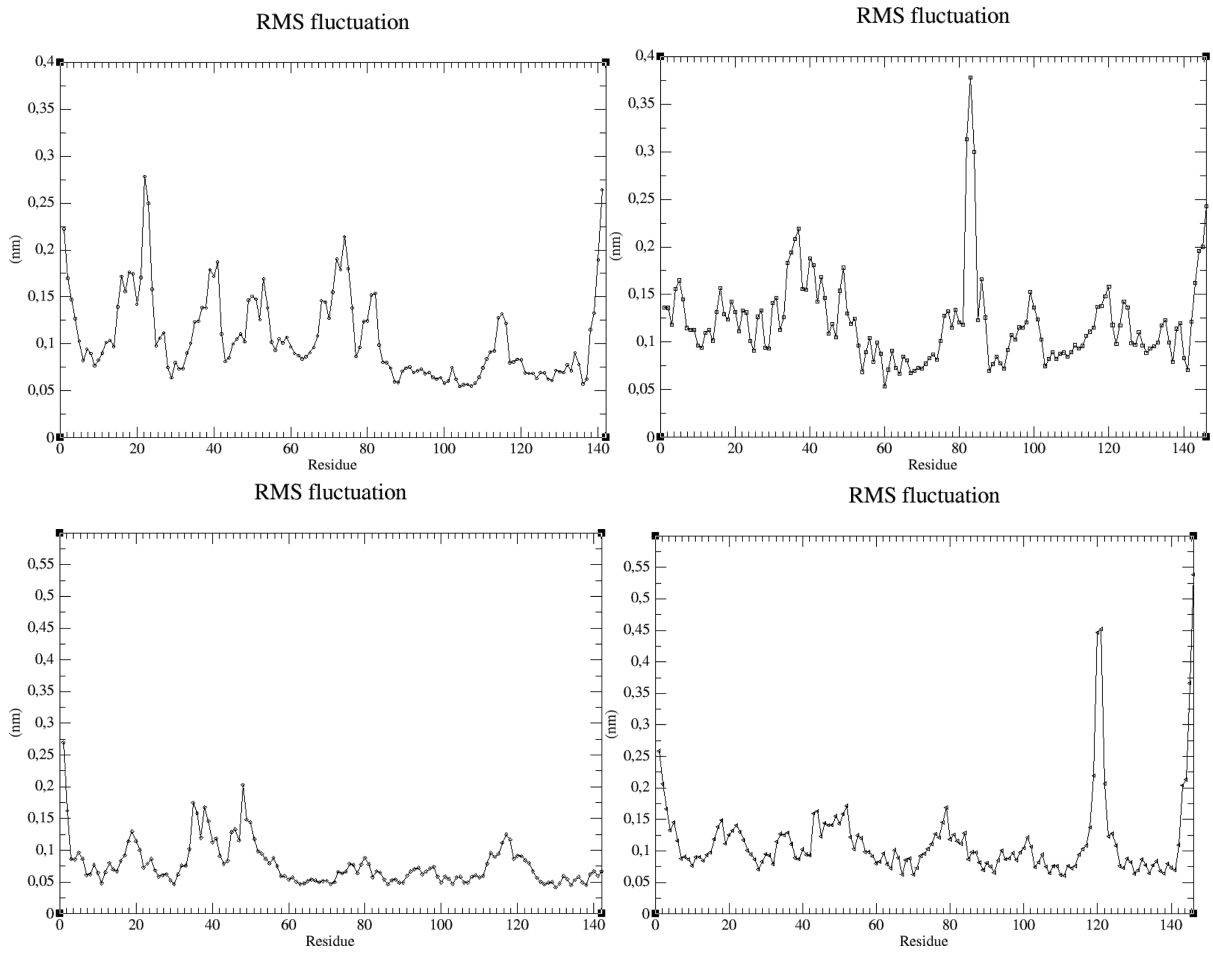


**Figure 4.** Root-mean-square fluctuations of $C^{\alpha}$ atoms for α- and β-chains of HbA (panel A and B) and HbTn (panel C and D, respectively).

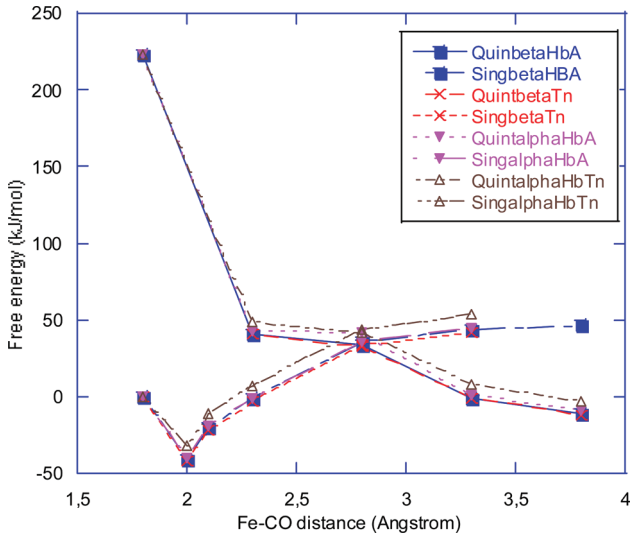


**Figure 5.** Single and quintet reaction free energy surface, as obtained by our PMM calculations for the α- (▼) and β-chains (□) of HbA and HbTn (× and ▲, for the α- and β-chain, respectively).

model involves: initial entry into the protein matrix, movement of the protein to allow the ligand to approach the binding site, and finally bond formation. Vice versa, at 300 K the CO initially bound at the heme iron overcomes these barriers after photodissociation and moves into the solvent.

In spite of very extensive investigations on the bond formation of CO to the heme of Mb,[24,50−52] a detailed characterization of the reaction pathway of CO binding to separated chains of

**TABLE 1: Free Energy Barrier for the Simulated Systems Compared to That Previously Determined for Myoglobin and in Vacuo Calculation**[a]

| ensemble | binding barrier (kJ/mol) | unbinding barrier (kJ/mol) |
|---|---|---|
| alpha *T. newnesi* Hb | 43.0 ± 0.2 | 72.8 ± 0.6 |
| alpha human Hb | 43.2 ± 0.2 | 73.1 ± 0.6 |
| beta T. *newnesi* Hb | 43.2 ± 0.2 | 73.0 ± 0.6 |
| beta human Hb | 43.4 ± 0.2 | 72.3 ± 0.6 |
| myoglobin[b] | 43.8 ± 0.6 | 74.1 ± 0.6 |
| in vacuo calculation[b] | 47.6 | 87.6 |

[a] The noise corresponds to a standard deviation. [b] From Amadei et al., 2007.[24]

human hemoglobin (HbA) is still missing. It should be recalled that the overall folding of these globins is similar, but the residues that form the heme pocket are quite different. For example, in the 10 Å radius of the α-chain HbA heme there are 3 His, 4 Phe, and 1 Tyr, whereas the β-chain features 2 His and 6 Phe. We have performed a computational study on the CO binding/unbinding to separated chains of HbA. Our results show that the free energy surfaces for the CO binding to separated chains of HbA are very similar to each other and that the kinetic constants are comparable. These data are in agreement with a number of experimental studies.[19] Furthermore, we have also performed a study on the CO binding/unbinding to the α- and β-chains of major Hb from *Trematomus newnesi* (HbTn). In the tetrameric structure, HbA and HbTn exhibit marked differences in their structural and biophysical properties.[25−29] Our results indicate that the dynamic behavior of HbTn

**TABLE 2: Rate Dissociation Constant for CO Binding to Separated α- and β-HbA Chains**

| ensemble | experimentally determined rate constant for CO dissociation $k_{off}$ ($s^{-1}$) | calculated $k_{unb}$ ($s^{-1}$) |
|---|---|---|
| α-chain of HbA | $0.012 \pm 0.001$[a] | 0.45[f] |
| | $0.005 \pm 0.002$[b] | |
| | $0.008 \pm 0.002$[c] | |
| | $0.012 \pm 0.001$[d] | |
| | $0.013 \pm 0.001$[e] | |
| β-chain of HbA | $0.007 \pm 0.001$[a] | |
| | $0.007 \pm 0.003$[b] | |
| | $0.011 \pm 0.002$[c] | |
| | $0.008 \pm 0.001$[d] | |
| | $0.008 \pm 0.001$[e] | 0.45[f] |

[a] From Unzai et al., 1998 (Cr, Mn, Ni, Mg hybrids).[19] [b] From Mathews et al., 1989.[58] [c] From Vandegriff et al., 1991.[59] [d] From Olson et al., 1987.[17] [e] From Giacometti et al., 1980.[60] [f] Noise evaluation provided 0.15−1.35 $s^{-1}$ as the total indetermination range for the rate constant.

chains is very similar to that of HbA chains and of myoglobin, suggesting that the CO binding to heme is not affected by the protein sequence and structure. This is probably due to the fact that all nonconservative replacements in the primary structure of the α- and β-chains of HbA and HbTn leave the electrostatic field surrounding the heme pocket essentially unmodified. In this respect, it can be concluded that the Fe−CO bond is mainly influenced by the position of the conserved distal histidine E7, which is the only residue reasonably close to the Fe−CO moiety.

These data leave unanswered the question of the differences in the oxidation rate and mechanism between HbA and HbTn, suggesting that an important role in defining these properties is played by the tetrameric structure.

The similar dynamic behavior of myoglobin, HbA, and HbTn chains is in agreement with the recent discovery that globins exhibit a high degree of correlated displacements, in particular in the C, E, and F helices.[22] In the globin family, sequence homology can be as small as 16%, but the fold is highly evolutionarily conserved.[30,31] Thus, the same structure in these proteins determines a similar dynamic behavior, at least in the functionally important regions, and assures the essential link structure/dynamics function.

It has been also proposed that although the features of CO binding to myoglobin are similar to those of isolated Hb chains the CO rebinding is faster in HbA chains than in myoglobin.[53] Our results suggest that the differences observed for the reaction with CO of these globins involve the rate of ligand migration to the solvent, rather than the Fe−CO complex formation/rupture. These findings are supported by recent works, both experimental and theoretical,[54−56] which focus on finding the CO ligand pathway inside globins. In particular, a very recent paper on the comparison of X-ray structures of globins in the presence of xenon has revealed that the location of the cavities is different from one globin to another.[54] Furthermore, computation of the complete map of the CO pathway inside a broad range of monomeric globins has shown that the location of these pathways can be very different for Mb's of different species[55] and for different globins.[56]

## Conclusion

In this paper, we have used molecular dynamics simulations, the perturbed matrix method, and basic statistical mechanics to describe the free energy surface and the kinetics of the reaction of CO binding/unbinding to separated HbA and HbTn chains. The rate constants describing this process are in reasonable agreement with available experimental data, further confirming the validity of this theoretical approach to the study of chemical reactions in complex systems. Interestingly, the data obtained for the separated chains of HbA and HbTn are very similar to each other and in good agreement with those reported for myoglobin. Accordingly, the binding of ligands to the heme in globins seems to follow a similar free energy surface, despite the structural differences within this protein family. The α/β equivalence found in the separated chains of the studied Hbs suggests that it is intrinsic to the chains and arises from evolutionary pressure to endow structurally inequivalent chains with the same functional properties.

Altogether our and previous data suggest that the differences observed in the kinetics among these proteins should be attributed to differences in the ligand migration from and to the solvent. This conclusion is supported by very recent experimental[54] and theoretical[55,56] data. Finally, our data provide an indirect support to the recent discovery that globin family proteins exhibit common dynamics,[22] further confirming previous observation that dynamic properties of proteins are strongly related to their overall architecture.[57]

**Acknowledgment.** This work was financially supported by PNRA (Italian National Programme for Antarctic Research) in the framework of the programme Evolution and Biodiversity in the Antarctic (EBA), sponsored by the Scientific Committee for Antarctic Research (SCAR) and by the Ministero Italiano dell'Università e della Ricerca Scientifica (PRIN 2007 "Struttura, funzione ed evoluzione di emoproteine da organismi marini artici ed antartici: meccanismi di adattamento al freddo e acquisizione di nuove funzioni").

## References and Notes

(1) Perutz, M. *Nature (London)* **1970**, *228*, 734.
(2) Mueser, T. C.; Rogers, P. H.; Arnone, A. *Biochemistry* **2000**, *39*, 15353.
(3) Schumacher, M. A.; Dixon, M. M.; Kluger, R.; Jones, R. T.; Brennan, R. G. *Nature* **1995**, *375*, 84.
(4) Schumacher, M. A.; Zheleznova, E. E.; Poundstone, K. S.; Kluger, R.; Jones, R. T.; Brennan, R. G. *Proc. Natl. Acad. Sci. U.S.A.* **1997**, *94*, 7841.
(5) Tame, J. R. H. *Trends Biochem. Sci.* **1999**, *24*, 372.
(6) Sanna, M. T.; Razynska, A.; Karavitis, M.; Koley, A. P.; Friedman, F. K.; Russu, I. M.; Brinigar, W. S.; Fronticelli, C. *J. Biol. Chem.* **1997**, *272*, 3478.
(7) Bucci, E.; Fronticelli, C. *Biochim. Biophys. Acta* **1971**, *243*, 170.
(8) Waks, M.; Yip, Y. K.; Beychok, S. *J. Biol. Chem.* **1973**, *248*, 6462.
(9) Yamaguchi, T.; Pang, J.; Reddy, K. S.; Witkowska, H. E.; Surrey, S.; Adachi, K. *J. Biol. Chem.* **1996**, *271*, 26677.
(10) Sugita, Y. *J. Biol. Chem.* **1975**, *250*, 1251.
(11) Asakura, T.; Adachi, K.; Sono, M.; Friedman, S.; Schwartz, E. *Biochem. Biophys. Res. Commun.* **1974**, *57*, 780.
(12) Brunori, M.; Noble, R. W.; Antonini, E.; Wyman, J. *J. Biol. Chem.* **1966**, *241*, 5238.
(13) Noble, R. W.; Gibson, Q. H.; Brunori, M.; Antonini, E.; Wyman, J. *J. Biol. Chem.* **1969**, *244*, 3905.
(14) Gibson, Q. H.; Ikeda-Saito, M.; Yonetani, T. *J. Biol. Chem.* **1985**, *260*, 14126.
(15) Geraci, G.; Parkhurst, L. J.; Gibson, Q. H. *J. Biol. Chem.* **1969**, *244*, 4664.
(16) Sharma, V. S.; Bandyopadhyay, D.; Berjis, M.; Rifkind, J.; Boss, G. R. *J. Biol. Chem.* **1991**, *266*, 24492.
(17) Olson, J. S.; Rohlfs, R. J.; Gibson, Q. H. *J. Biol. Chem.* **1987**, *262*, 12930.
(18) Hernan, R. A.; Sligar, S. G. *J. Biol. Chem.* **1995**, *270*, 26257.
(19) Yokoyama, T.; Chong, K. T.; Miyazaki, G.; Morimoto, H.; Shih, D. T. B.; Unzai, S.; Tame, J. R. H.; Park, S.-Y. *J. Biol. Chem.* **2004**, *279*, 28632.
(20) Amadei, A.; D'Alessandro, M.; Aschi, M. *J. Phys. Chem. B* **2004**, *108*, 16250.
(21) Alcantara, R. E.; Xu, C.; Spiro, T. G.; Guallar, V. *Proc. Natl. Acad. Sci. U.S.A.* **2007**, *104*, 18451.

(22) Ma, J. G.; Laberge, M.; Song, X. Z.; Jentzen, W.; Jia, S. L.; Zhang, J.; Vanderkooi, J. M.; Shelnutt, J. A. *Biochemistry* **1998**, *37*, 5118.
(23) Boechi, L.; Mañez, P. A.; Luque, F. J.; Marti, M. A.; Estrin, D. A. *Proteins* **2010**, *78*, 962.
(24) Amadei, A.; D'Abramo, M.; Daidone, I.; D'Alessandro, M.; Di Nola, A.; Aschi, M. *Theor. Chem. Acc.* **2007**, *117*, 637.
(25) Vergara, A.; Vitagliano, L.; Verde, C.; di Prisco, G.; Mazzarella, L. *Methods Enzymol.* **2008**, *436*, 425.
(26) Vitagliano, L.; Bonomi, G.; Riccio, A.; di Prisco, G.; Smulevich, G.; Mazzarella, L. *Eur. J. Biochem.* **2004**, *271*, 1651.
(27) Riccio, A.; Vitagliano, L.; di Prisco, G.; Zagari, A.; Mazzarella, L. *Proc. Natl. Acad. Sci. U.S.A.* **2002**, *99*, 9801.
(28) Vitagliano, L.; Vergara, A.; Bonomi, G.; Merlino, A.; Verde, C.; di Prisco, G.; Howes, B. D.; Smulevich, G.; Mazzarella, L. *J. Am. Chem. Soc.* **2008**, *130*, 10527.
(29) Merlino, A, V. L.; Howes, B. D.; Verde, C.; di Prisco, G.; Smulevich, G.; Sica, F.; Vergara, A. *Biopolymers.* **2009**, *91*, 1117.
(30) Chothia, C.; Lesk, A. M. *Protein Folding, Proc. Conf. Ger. Biochem. Soc., 28th* **1980**, 63.
(31) Bashford, D.; Chothia, C.; Lesk, A. M. *J. Mol. Biol.* **1987**, *196*, 199.
(32) Van Der Spoel, D.; Lindahl, E.; Hess, B.; Groenhof, G.; Mark, A. E.; Berendsen, H. J. *J. Comput. Chem.* **2005**, *26*, 1701.
(33) Park, S.-Y.; Yokoyama, T.; Shibayama, N.; Shiro, Y.; Tame, J. R. H. *J. Mol. Biol.* **2006**, *360*, 690.
(34) Mazzarella, L.; D'Avino, R.; di Prisco, G.; Savino, C.; Vitagliano, L.; Moody, P. C. E.; Zagari, A. *J. Mol. Biol.* **1999**, *287*, 897.
(35) Berendsen, H. J. C.; Postma, J. P. M.; van Gusteren, W. F.; Hermans, J. *Dordrecht: Reidel* **1981**, 331.
(36) Kerwin, B. A.; Looker, D. G.; Hess, E.; Revilla-Sharp, P.; Akers, M. J. *Book of Abstracts, 213th ACS National Meeting*, San Francisco, April 13−17, 1997, I&EC.
(37) Darden, T.; York, D.; Pedersen, L. *J. Chem. Phys.* **1993**, 10089.
(38) Berendsen, H. J. C.; Postma, J. P. M.; van Gusteren, W. F.; Di Nola, A.; Haak, J. R. *J. Chem. Phys.* **1984**, *81*, 3684.
(39) Amadei, A.; Ceruso, M. A.; Di Nola, A. *Proteins* **1999**, *36*, 419.
(40) Merlino, A.; Vitagliano, L.; Ceruso, M. A.; Di Nola, A.; Mazzarella, L. *Biopolymers* **2002**, *65*, 274.
(41) Ceruso, M. A.; Amadei, A.; Di Nola, A. *Protein Sci.* **1999**, *8*, 147.
(42) Merlino, A.; Vitagliano, L.; Ceruso, M. A.; Mazzarella, L. *Biophys. J.* **2004**, *86*, 2383.
(43) Merlino, A.; Ceruso, M. A.; Vitagliano, L.; Mazzarella, L. *Biophys. J.* **2005**, *88*, 2003.
(44) Amadei, A.; de Groot, B. L.; Ceruso, M. A.; Paci, M.; Di Nola, A.; Berendsen, H. J. *Proteins* **1999**, *35*, 283.
(45) Frisch, M. J.; Trucks, G. W.; Schlegel, H. B.; Scuseria, G. E.; Robb, M. A.; Cheeseman, J. R.; Montgomery, J. A., Jr.; Vreven, T.; Kudin, K. N.; Burant, J. C.; Millam, J. M.; Iyengar, S. S.; Tomasi, J.; Barone, V.; Mennucci, B.; Cossi, M.; Scalmani, G.; Rega, N.; Petersson, G. A.; Nakatsuji, H.; Hada, M.; Ehara, M.; Toyota, K.; Fukuda, R.; Hasegawa, J.; Ishida, M.; Nakajima, T.; Honda, Y.; Kitao, O.; Nakai, H.; Klene, M.; Li, X.; Knox, J. E.; Hratchian, H. P.; Cross, J. B.; Bakken, V.; Adamo, C.; Jaramillo, J.; Gomperts, R.; Stratmann, R. E.; Yazyev, O.; Austin, A. J.; Cammi, R.; Pomelli, C.; Ochterski, J. W.; Ayala, P. Y.; Morokuma, K.; Voth, G. A.; Salvador, P.; Dannenberg, J. J.; Zakrzewski, V. G.; Dapprich, S.; Daniels, A. D.; Strain, M. C.; Farkas, O.; Malick, D. K.; Rabuck, A. D.; Raghavachari, K.; Foresman, J. B.; Ortiz, J. V.; Cui, Q.; Baboul, A. G.; Clifford, S.; Cioslowski, J.; Stefanov, B. B.; Liu, G.; Liashenko, A.; Piskorz, P.; Komaromi, I.; Martin, R. L.; Fox, D. J.; Keith, T.; Al-Laham, M. A.; Peng, C. Y.; Nanayakkara, A.; Challacombe, M.; Gill, P. M. W.; Johnson, B.; Chen, W.; Wong, M. W.; Gonzalez, C.; Pople, J. A. *Gaussian 03*, revision C.02; Gaussian, Inc.: Wallingford, CT, 2004.
(46) Schmidt, K. K. B., M. W.; Boatz, J. A.; Elbert, S. T.; Gordon, M. S.; Jensen, J. H.; Koseki, S.; Matsunaga, N.; Nguyen, K. A.; Su, S.; Windus, T. L.; Dupuis, M.; Montgomery, J. A. *J. Comput. Chem.* **1993**, *14*, 1347.
(47) Lee, C. Y., W.; Parr, R. G. *Phys. Rev. B* **1988**, *37*, 785.
(48) Hay, P. J.; Wadt, W. R. *J. Chem. Phys.* **1985**, *82*, 270.
(49) Song, X. J.; Yuan, Y.; Simplaceanu, V.; Sahu, S. C.; Ho, N. T.; Ho, C. *Biochemistry* **2007**, *46*, 6795.
(50) Bourgeois, D.; Vallone, B.; Arcovito, A.; Sciara, G.; Schotte, F.; Anfinrud, P. A.; Brunori, M. *Proc. Natl. Acad. Sci. U.S.A.* **2006**, *103*, 4924.
(51) Sottini, S.; Abbruzzetti, S.; Viappiani, C.; Ronda, L.; Mozzarelli, A. *J. Phys. Chem. B* **2005**, *109*, 19523.
(52) Sottini, S.; Abbruzzetti, S.; Spyrakis, F.; Bettati, S.; Ronda, L.; Mozzarelli, A.; Viappiani, C. *J. Am. Chem. Soc.* **2005**, *127*, 17427.
(53) Alberding, N.; Chan, S. S.; Eisenstein, L.; Frauenfelder, H.; Good, D.; Gunsalus, I. C.; Nordlund, T. M.; Perutz, M. F.; Reynolds, A. H.; Sorensen, L. B. *Biochemistry* **1978**, *17*, 43.
(54) Savino, C, M. A.; Draghi, F.; Johnson, K. A.; Sciara, G.; Brunori, M.; Vallone, B. *Biopolymers* **2009**, *91*, 1097.
(55) Cohen, J.; A., A.; Braun, R.; Schulten, K. *Biophys. J.* **2006**, *91*, 1844.
(56) Cohen, J.; K., S. *Biophys. J.* **2007**, *93*, 3591.
(57) Merlino, A.; Vitagliano, L.; Ceruso, M. A.; Mazzarella, L. *Proteins* **2003**, *53*, 101.
(58) Mathews, A. J.; Rohlfs, R. J.; Olson, J. S.; Tame, J.; Renaud, J. P.; Nagai, K. *J. Biol. Chem.* **1989**, *264*, 16573.
(59) Kaca, W.; Roth, R. I.; Vandegriff, K. D.; Chen, G. C.; Kuypers, F. A.; Winslow, R. M.; Levin, J. *Biochemistry* **1995**, *34*, 11176.
(60) Giacometti, G. M.; Brunori, M.; Antonini, E.; Di Iorio, E. E.; Winterhalter, K. H. *J. Biol. Chem.* **1980**, *255*, 6160.

JP908525S